Solar MHD Theory and Observations: A High Spatial Resolution Perspective
ASP Conference Series, Vol. 354, 2006
Uitenbroek, Leibacher, and Stein

Magnetic Patches in Internetwork Areas

A. G. de Wijn,[1] R. J. Rutten,[1,2] E. M. W. P. Haverkamp,[1] and P. Sütterlin[1]

[1]*Sterrekundig Instituut, Utrecht University, Postbus 80 000, 3508 TA Utrecht, The Netherlands*

[2]*Institute of Theoretical Astrophysics, Oslo University, P.O. Box 1029 Blindern, N-0315 Oslo, Norway*

Abstract. We present a study of internetwork magnetic elements that appear as bright points in G-band (photosphere) and Ca II H (low chromosphere) image sequences from the Dutch Open Telescope. Many bright points appear intermittently in groups of long-lived structures that we call "magnetic patches". We develop an algorithm for the identification of bright points and magnetic patches. The average internetwork bright point lifetimes is measured to be 3.5 minutes in the G band, and 4.3 minutes in the Ca II H. We find an internetwork bright point number density of 0.02 Mm^{-2} in the G-band sequence and 0.05 Mm^{-2} in the Ca II H sequence. The bright points show a bimodal distribution of the frame-to-frame horizontal velocities, with a peak at 0 $\mathrm{km\,s}^{-1}$ and a wide hump centered around 1.2 $\mathrm{km\,s}^{-1}$. The patches last much longer than granular time scales (about nine hours) and outline cell-like structures on mesogranular scale. We conclude that transient internetwork bright points trace the locations of strong magnetic fields that exist before the bright point appears and remain after it disappears.

1. Introduction

Magnetic elements observed in, *e.g.*, G-band images, appear as bright points in internetwork areas of the quiet Sun. They closely resemble network bright points (NBPs) that have been studied extensively with the former and present Swedish Solar Telescope (Berger et al. 1995, 2004; Rouppe van der Voort et al. 2005). Magnetism in quiet-Sun internetwork areas has not been studied as intensively. Recently however, it has come under intense scrutiny (*e.g.*, Domínguez Cerdeña et al. 2003; Sánchez Almeida et al. 2003; Socas-Navarro & Lites 2004; Trujillo Bueno et al. 2004; Manso Sainz et al. 2004). Magnetic fields with field strengths ranging from less than a hundred to over a kiloGauss seem to permeate the internetwork at small spatial scales. As expected, stronger fields collect in intergranular lanes, and may form internetwork bright points (IBPs) when strong enough to be evacuated sufficiently in the low photosphere. Though not all magnetic features produce observable bright points (Berger & Title 2001), they serve well as tracers of strong-field magnetic elements, especially in the Fraunhofer G band (CH lines around 430.5 nm) and the CN band at 388 nm (*cf.* Rutten, Kiselman, Rouppe van der Voort, & Plez 2001).

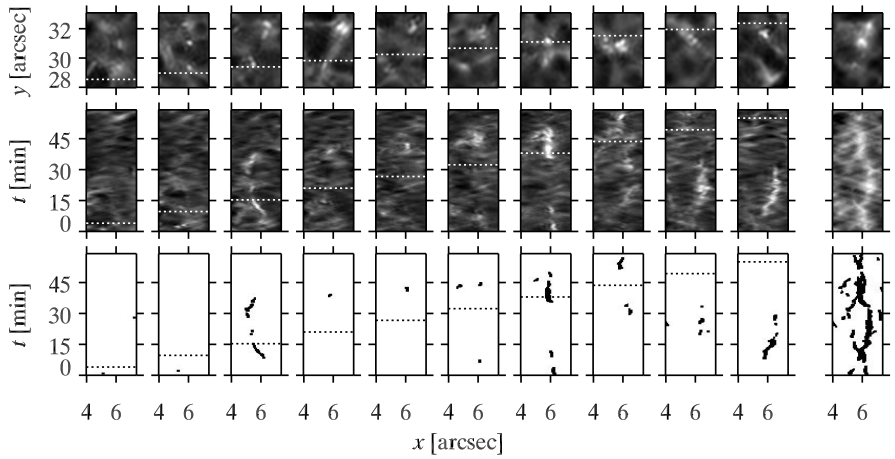

Figure 1. Example of a magnetic patch, visualized by partial Ca II H images (x-y cutouts, top row), the associated Ca II H x-t slices (middle row), and the corresponding x-t slices from the IBP map sequence (bottom row). The rightmost panels are averages over all data collected in the one-hour duration of the sequence (top panel) or in the y interval shown here (lower panels). The y location of each x-t slice is shown by a dashed line in the associated x-y panel, while the time of the latter is shown by a dashed line in the corresponding x-t slice.

We analyze synchronous G-band and Ca II H image sequences with high resolution and fast cadence to study the lifetimes of IBPs. Rutten et al. (2004) remarked that an IBP persisted as a magnetic flasher over the full 54-minute sequence. The main issue discussed here is whether briefly appearing IPBs systematically reveal longer-lived flux concentrations.

2. Observations, Data Reduction, and Patch Identification

We use a double image sequence recorded by the Dutch Open Telescope (DOT). We recorded synchronous images in the Fraunhofer G band and in Ca II H at line center from 8:40 to 9:39 UT at a 20-second cadence. Details on the data, alignment, and filtering, including a set of sample images, can be found in de Wijn et al. (2005).

A three-dimensional "cube slicer" is an ideal tool to visually inspect these data. The cube slicer dissects both cubes simultaneously in x-y, x-t, and y-t slices with continuous (x, y, t) selection controlled by mouse movement. Slow scanning through the cubes at the location of an IBP often reveals a "magnetic patch": a structure composed of many IBPs that appear intermittently. These structures can consist of multiple tracks of IBPs that merge and split during the sequence.

The example shown in Figure 1 mimics the cube slicer by showing a sequence of small image (top row) and slice (middle row) cutouts at several t and y locations. The rightmost column displays the average over t (top panel) and y (middle panel). We discuss the appearance of the bright IBP near $y \approx 31''$

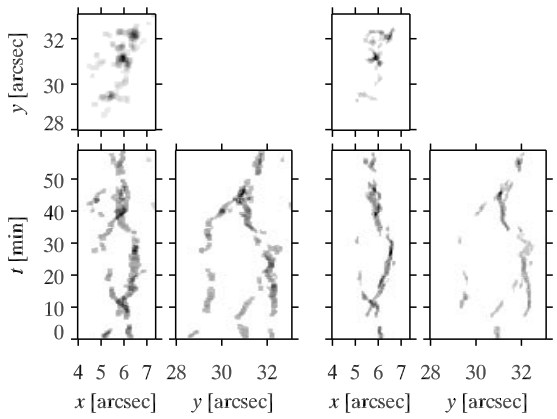

Figure 2. Integrated x-y cutout, and x-t and y-t slices corresponding to those in Figure 1 of the binary IBP map sequences for the Ca II H (*left*) and G band (*right*), showing only those IBPs that group into the central patch. Careful comparison with the rightmost panel in the bottom row of Figure 1 shows that several IBPs present there are part of another patch, such as at the leftmost edge of the cutout around $t \approx 25$ minutes. IBP map sequence over the missing third coordinate.

in the seventh x-y panel for $t \approx 38$ minutes. From the single slice, it appears stable during its 15-minute lifetime, appearing and disappearing abruptly. Cube slicing, however, shows that the enhanced brightness nearby in y before and after this slice is part of the same IBP.

The bottom row of Figure 1 displays the result of our IBP detection algorithm. For the sake of brevity, we omit a detailed description here, and refer reader to Section 2 of de Wijn et al. (2005). The rightmost panel shows that the algorithm recovers much of the brightness pattern. Some IBPs detected by the algorithm are not visible in the average x-t slice, for example those around $x \approx 5''$ and $t \approx 20$ minutes.

We define two IBPs that have a minimum separation of less than $0.71''$, disregarding temporal information, as friends, and apply a friends-of-friends algorithm to form connected groups of IBPs that have no friends outside the group. Through this procedure, each IBP is associated with a single patch. Patches, however, may contain multiple IBPs.

We visualize the three-dimensional structure of our example patch of Figure 1 in Figure 2. This particular patch is made up of 24 IBPs in the Ca II H IBP map. Since not all IBPs identified in Figure 1 are members of this patch, some IBPs identified there are missing here.

3. Results and Discussion

In total, our processing identifies 387 IBPs in 149 patches in the G-band sequence, and 848 IBPs in 217 patches in the Ca II H sequence. The algorithm is able to detect more IBPs in the Ca II H data than in the G-band data, due to the increased brightness enhancement of the IBPs against the surrounding. Of

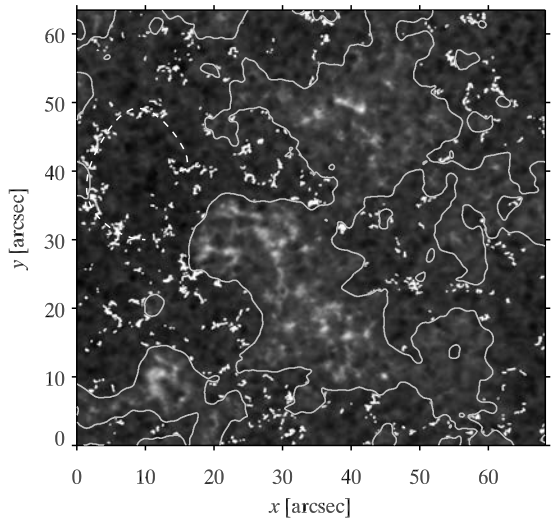

Figure 3. The average Ca II H image with IBPs identified in the Ca II H sequence overlaid in white. The IBPs appear to group in patches that outline edges of cell-like structures, such as around $(x, y) = (10\,''\!, 40'')$ (indicated by a dashed line). The gray contour indicates the shape of the internetwork mask.

the G-band patches, 85% have a corresponding Ca II H patch, and 76 G-band and 125 Ca II H patches contain multiple IBPs.

Figure 3. shows the mask of the Ca II H IBP locations. They are arranged in a striking pattern at the borders of cell-like structures of mesogranular scale. A large, conspicuous cell centered around $(x, y) = (10'', 40'')$ is marked with a dashed curve. Many more cells are easily identified by eye, *e.g.*, around $(28'', 40'')$ and $(20'', 15'')$. Several earlier studies on internetwork magnetograms have reported similar patterns (Domínguez Cerdeña et al. 2003; Sánchez Almeida 2003; Domínguez Cerdeña 2003). Photospheric flows are expected to be the cause of these patterns, and indeed they have been shown to exist in studies by, *e.g.*, Krijger & Roudier (2003) and Roudier & Muller (2004).

We measure the IBP lifetimes in the G band and in Ca II H and find 3.5 and 4.3 minutes on average, with a long tail towards long lifetimes. Network bright points have much longer lifetimes. Berger et al. (1998) report an average of 9.3 minutes for G-band NBPs. Their data processing methods differ from ours. It is likely that they can identify and track G-band bright points better. However, our results from the Ca II H sequence suggest that IBPs truly have shorter lifetimes than NBPs. The strong fields in network areas cause "abnormal granulation" by fragmenting granules. This gives flux tubes in network areas a relatively quiet existence as compared to in internetwork areas. It seems likely that the continuous buffeting by granules disturbs the processes that make IBPs bright in G-band images, but also in Ca II H. From the IBP patterns we observe, we conclude that transient IBPs trace the locations of strong magnetic fields that existed before the IBPs appear and which remain after the IBPs disappear. This conclusion is supported by the results of Berger & Title (2001), who show that

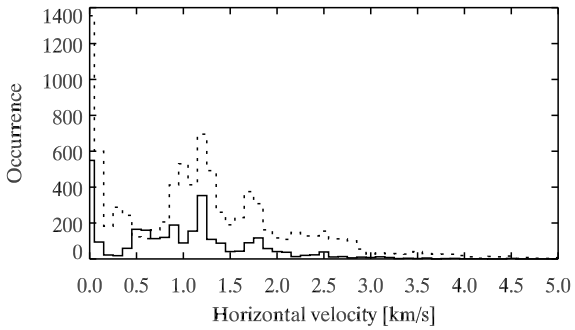

Figure 4. Horizontal velocities derived from the frame-to-frame motion of the center of mass of individual IBPs in the G band (solid) and in Ca II H (dashed). Both histograms display a peak at 0 $\mathrm{km\,s^{-1}}$ and a wide hump around 1.2 $\mathrm{km\,s^{-1}}$.

magnetism, though necessary, is not a sufficient condition for formation of a network bright point.

We measure the horizontal speeds of all IBPs by computing the displacement of the center of gravity of the IBP in two successive frames. Figure 4 shows the resulting speeds. The distribution shows a peak at 0 $\mathrm{km\,s^{-1}}$ and a wide hump around 1.2 $\mathrm{km\,s^{-1}}$, both in the G band and in the Ca II H sequence. Inspection of individual IBPs shows that single IBPs mix both velocities, but avoid speeds around 0.5 $\mathrm{km\,s^{-1}}$. This result differs from speeds derived for NBPs by Berger et al. (1998) and by Nisenson et al. (2003). Possibly IBPs are more restricted by the stronger granulation, allowing only fast IBP movement along the intergranular lanes and collecting them at the stable intersections.

The average IBP number density in internetwork areas is 0.02 $\mathrm{Mm^{-2}}$ in the G-band sequence and 0.05 $\mathrm{Mm^{-2}}$ in the Ca II H sequence. Sánchez Almeida et al. (2004) find a much higher density of 0.3 $\mathrm{Mm^{-2}}$ in their best G-band image. Because of the higher resolution of their data, and because of their manual search, it is likely they can identify smaller and fainter features than our conservative algorithm. Their field of view also contains a small network patch, in and around which the number density of bright points is obviously increased. If our value is a lower limit, theirs is an upper limit on the true IBP number density.

The patch in Figure 2 is visible for the entire duration of the sequence. Only a few patches begin and end within the duration of the sequence. This suggests that their typical lifetime is much larger than the duration of the sequence. A statistical analysis can be used to obtain an estimate for the average patch lifetime. The details of the analysis are discussed in Section 3.3 of de Wijn et al. (2005). We compare the observed number of patches that persist through the entire sequence, the number of patches that emerge as well as disappear during the sequence, and the number of patches that either emerge or disappear within the duration of the sequence to the values expected for an exponential distribution of patch lifetimes. We find an average lifetime of 530 ± 50 minutes.

4. Conclusion

Our analysis has identified many IBPs in quiet-Sun internetwork cells. We attribute both IBPs in the G-band and Ca II H sequences to strong, kiloGauss magnetic elements. We measured the IBP number density and find a significantly lower value than Sánchez Almeida et al. (2004). The difference can likely be explained by the lower resolution of our data, and by our more conservative identification criteria. We computed frame-to-frame velocities for the IBPs and found a distribution with a peak around 0 $\mathrm{km\,s^{-1}}$ and a wide hump centered around 1.2 $\mathrm{km\,s^{-1}}$. Individual IBPs show periods of rapid motion and periods of stability. The nature of this distribution requires further study. We found that the IBPs appear in patches that outline cell-like structures, that we believe are the magnetic-element voids connected to mesogranular upwelling found by Domínguez Cerdeña et al. (2003). We determined the average IBP patch lifetime to be about nine hours. This is long enough for the magnetic elements in a patch to assemble at mesogranular vertexes. The long lifetime is an indication that strong internetwork magnetic fields are unlikely to be caused by a granular dynamo as discussed by, *e.g.*, Cattaneo (1999).

Acknowledgments. The DOT is operated by Utrecht University at the Spanish Observatorio del Roque de los Muchachos of the Instituto de Astrofísica de Canarias and is presently funded by Utrecht University, the Netherlands Organisation for Scientific Research NWO, NOVA, and SOZOU.

References

Berger, T. E., Löfdahl, M. G., Shine, R. S., & Title, A. M. 1998, ApJ, 495, 973
Berger, T. E., Rouppe van der Voort, L. H. M., Löfdahl, M. G., et al. 2004, A&A, 428, 613
Berger, T. E., Schrijver, C. J., Shine, R. A., et al. 1995, ApJ, 454, 531
Berger, T. E. & Title, A. M. 2001, ApJ, 553, 449
Cattaneo, F. 1999, ApJ, 515, L39
de Wijn, A. G., Rutten, R. J., Haverkamp, E. M. W. P., & Sütterlin, P. 2005, A&A, 441, 1183
Domínguez Cerdeña, I. 2003, A&A, 412, L65
Domínguez Cerdeña, I., Kneer, F., & Sánchez Almeida, J. 2003, ApJ, 582, L55
Krijger, J. M. & Roudier, T. 2003, A&A, 403, 715
Manso Sainz, R., Landi Degl'Innocenti, E., & Trujillo Bueno, J. 2004, ApJ, 614, L89
Nisenson, P., van Ballegooijen, A. A., de Wijn, A. G., & Sütterlin, P. 2003, ApJ, 587, 458
Roudier, T. & Muller, R. 2004, A&A, 419, 757
Rouppe van der Voort, L. H. M., Hansteen, V. H., Carlsson, M., et al. 2005, A&A, 435, 327
Rutten, R. J., de Wijn, A. G., & Sütterlin, P. 2004, A&A, 416, 333
Rutten, R. J., Kiselman, D., Rouppe van der Voort, L., & Plez, B. 2001, in ASP Conf. Ser. Vol. 236: Advanced Solar Polarimetry - Theory, Observation, and Instrumentation, ed. M. Sigwarth (San Francisco: ASP), 445
Sánchez Almeida, J. 2003, A&A, 411, 615
Sánchez Almeida, J., Domínguez Cerdeña, I., & Kneer, F. 2003, ApJ, 597, L177
Sánchez Almeida, J., Márquez, I., Bonet, J. A., Domínguez Cerdeña, I., & Muller, R. 2004, ApJ, 609, L91
Socas-Navarro, H. & Lites, B. W. 2004, ApJ, 616, 587
Trujillo Bueno, J., Shchukina, N., & Asensio Ramos, A. 2004, Nat, 430, 326